

2'-O-methylation and N6-methyladenosine enhance the oral delivery of small RNAs in mice

Shaoting Guo,^{1,4} Zhen Li,^{1,4} Xiaobei Li,¹ Zhu Liang,^{1,2,3} Dandan Zhao,¹ Na Sun,¹ Jiaqi Liu,¹ Xiaona Wang,¹ Song Mei,¹ Xiangyu Qiao,¹ and Chengyu Jiang¹

¹State Key Laboratory of Common Mechanism Research for Major Diseases, Institute of Basic Medical Sciences, Chinese Academy of Medical Sciences & Peking Union Medical College, Beijing 10000, China

Studies have demonstrated that small RNAs originating from plants can be taken up by the human digestive system and play a role in regulating gene expression. However, the impact of naturally occurring RNA modifications in these small RNAs on their absorption has been underexplored. Here, we show that 2'-O-methylation (2'-O-Me), N6-methyladenosine (m⁶A), and 5-methylcytidine (m⁵C) exhibit high abundance in small RNAs (18–30 nt) derived from herbal decoction. 2'-O-Me and m⁶A promote the oral delivery of small RNAs *in vitro* and *in vivo*, whereas m⁵C did not show the same enhancement. To study the underlying mechanism of this enhancement, we used liposomes to simulate the negatively charged cell membrane and investigated the influence of these modifications on RNA-biomembrane interaction, independent of RNA stability. Our findings provide a novel perspective on the role of modifications in small RNAs, offering insights into their potential applications in oral delivery for oligonucleotides.

INTRODUCTION

Despite the challenges posed by the hydrophilic and unstable nature of RNAs, research suggests that small plant-derived RNAs are absorbed by mammals through the gastrointestinal tract and can influence gene regulation.^{1–5} In a previous study conducted in our laboratory, a large-scale analysis revealed a substantial presence of unique small RNAs in both traditional Chinese medicine (TCM) decoctions and blood samples from individuals who had consumed herbal decoctions.² Notably, certain small RNAs derived from plants have demonstrated therapeutic effects in the treatment of human diseases.^{6–9} This finding underscores the potential significance of these small RNAs in the context of traditional medicine practices. Natural modifications on small RNAs can significantly alter their physicochemical properties, potentially contributing to the high abundance of small RNAs even after exposure to the high-temperature processing of decoctions, thereby influencing their oral delivery.

Naturally occurring RNA modifications have provided valuable insights for the development of mRNA vaccines and oligonucleotide drugs.^{10–12} To date, more than 170 distinct RNA modifications

have been identified across various RNA species, with particular emphasis on tRNA, rRNA, and mRNA.¹³ One notable modification is the introduction of pseudouridine to mRNA, which has been shown to enhance translational efficiency and reduce its immunogenicity *in vivo*.¹⁴ Another significant modification is 2'-O-Me, naturally present at the 3' terminal ribose of plant microRNAs.¹⁵ The number of 2'-O-Me correlates with increased thermostability and biological stability of small RNAs.^{16,17} This modification is widely employed in antisense oligonucleotide (ASO) drugs. Currently, therapeutic oligonucleotides are primarily administered via intravenous injection, subcutaneous injection, or local injection. Several pioneering studies have investigated the feasibility of oral delivery for oligonucleotide-based therapeutics.^{18–21} Exploring the role of naturally occurring RNA modifications in the oral delivery of plant-derived small RNAs may offer insights for the development of orally administered oligonucleotides.

Chemical modifications are commonly used to enhance RNA stability against RNase degradation, yet they can also affect RNA delivery independently of stability. Phosphorothioate (PS) modification, widely employed in approved oligonucleotide therapeutics, not only robustly increases RNA's resistance to RNase but also improves its affinity for proteins such as epidermal growth factor receptor (EGFR) and the Stabilin class of scavenger receptors, facilitating rapid PS-ASO adsorption and internalization.^{22–24} Moreover, conjugation of N-acetyl galactosamine (GalNac) is crucial for liver-targeted delivery of ASO and small interfering RNA (siRNA). This is achieved by enhancing their interaction

Received 10 August 2024; accepted 21 May 2025;
<https://doi.org/10.1016/j.omtn.2025.102574>

²Present address: Zhu Liang, Chinese Academy for Medical Sciences Oxford Institute, Nuffield Department of Medicine, University of Oxford, Roosevelt Drive, Oxford OX3 7FZ, UK

³Present address: Zhu Liang, Target Discovery Institute, Centre for Medicines Discovery, Nuffield Department of Medicine, University of Oxford, Roosevelt Drive, Oxford OX3 7FZ, UK

⁴These authors contributed equally

Correspondence: Chengyu Jiang, State Key Laboratory of Common Mechanism Research for Major Diseases, Institute of Basic Medical Sciences, Chinese Academy of Medical Sciences & Peking Union Medical College, Beijing 10000, China.

E-mail: jiang@pumc.edu.cn



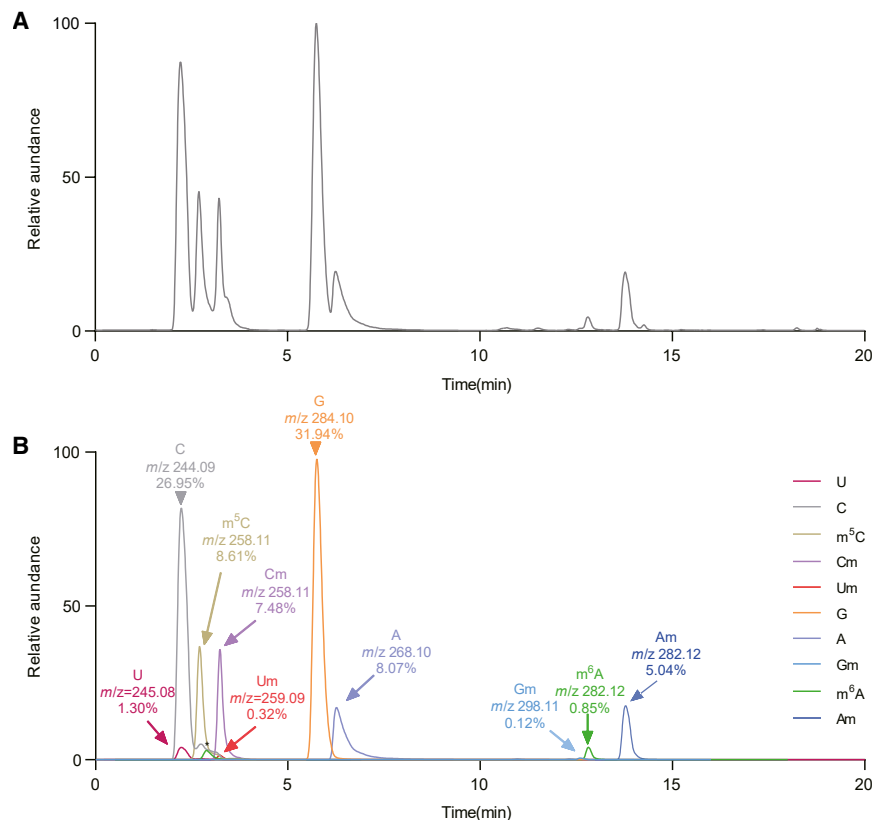


Figure 1. LC-MS-based analysis of RNA modifications in small RNAs derived from herbal decoction

(A) Total ion chromatograms (TIC) detecting the single nucleosides of small RNAs (18–30 nt) derived from BZL decoction. (B) Super-imposed extracted ion chromatograms (EIC) detecting proton adducts of unmodified and modified nucleosides. The relative content (%) of the interested nucleosides is provided. Asterisks indicate unassigned ions. Extracted ion chromatogram of each nucleoside is provided in Figure S3. Am, 2'-O-methyladenosine; m⁶A, N6-methyladenosine; m⁵C, 5-methylcytosine; Cm, 2'-O-methylcytosine; Um, 2'-O-methyluridine; Gm, 2'-O-methylguanosine.

with the asialoglycoprotein receptor (ASGR), leading to internalization through clathrin-dependent receptor-mediated endocytosis.^{25,26} While majority of studies on RNA absorption focus on its interaction with proteins, there is a notable gap in research concerning RNA interactions with lipid bilayers in biomembranes. Permeability is the major obstacle for the oral delivery of oligonucleotides.¹⁸ Both DNA and RNA exhibit nonspecific and weak interactions with phospholipid membranes.²⁷ RNA binding to liposomes has been shown to enhance liposome permeability.²⁸ Furthermore, supramolecular RNA complexes can disrupt phospholipid bilayers, leading to the release of liposome-encapsulated solutes.²⁹ RNA-lipid interactions involve the electrostatic interactions between the phosphate back bone and lipid head, as well as hydrophobic interactions between nucleobases and lipid tails.^{30,31} RNAs with high guanine content and double-stranded structures exhibit increased binding efficiency.³² RNA modification introduces changes to the electrostatic charge and hydrophobic surface of RNA,¹² potentially influencing its interaction with biomembranes. This alteration in RNA characteristics may influence RNA absorption efficiency, as increased RNA binding to the cell membrane implies a higher effective concentration at the cell surface.

In this study, we detected a high abundance of 2'-O-methylnucleotide, N6-methyladenosine, and 5-methylcytosine in small RNAs

(18–30 nt) derived from herbal decoction and focused on their influence on RNA uptake. Our findings revealed that 2'-O-Me demonstrated a robust capacity to enhance small RNA oral delivery *in vitro* and *in vivo*. 2'-O-Me increased the binding of small RNAs to liposomes that simulate the negatively charged cell membrane. Remarkably, 2'-O-Me facilitated small RNA penetration of the lipid bilayer under low pH condition. m⁶A exhibited similar effects to 2'-O-Me, whereas m⁵C did not show the same enhancement. Our results revealed the mechanisms by which 2'-O-Me and m⁶A assist small RNAs in traversing the gastrointestinal tract, emphasizing the pivotal roles of improved biomembrane-RNA interaction.

RESULTS

Detection of RNA modifications in plant-derived small RNAs

RNA is generally considered unstable in the digestive system, yet small RNAs derived from plants can be absorbed through oral administration and mediate cross-kingdom regulation.^{7,9} Previous studies in our laboratory identified the presence of exosome-like nanoparticles, referred to as decoctosomes, in traditional Chinese medicinal decoctions.⁷ These nanoparticles consist of lipids, proteins, small chemical molecules, and small RNAs. Decoctosomes may provide a protective barrier that shields small RNAs from degradation. Furthermore, small RNAs with secondary structures tend to exhibit greater stability compared to those that are unstructured,³³ which could also be a crucial factor in enhancing the survival of small RNAs. Natural RNA modifications on these small RNAs may also help them survive the high-temperature process of decoction and the hostile digestive environment. This study focused on quantifying 2'-O-Me, m⁶A, and m⁵C in 18–30 nt small RNAs from Ban Zhi Lian (*Scutellaria barbata*), a traditional Chinese herb (Figures S1A and Figure S2). The relative content of each nucleotide was calculated based on the liquid chromatography-mass spectrometry (LC-MS) results (Figure 1; Figure S3). 2'-O-Me is common in coding and non-coding RNA, involving methylation at the 2'O position in the ribose sugar moiety across all

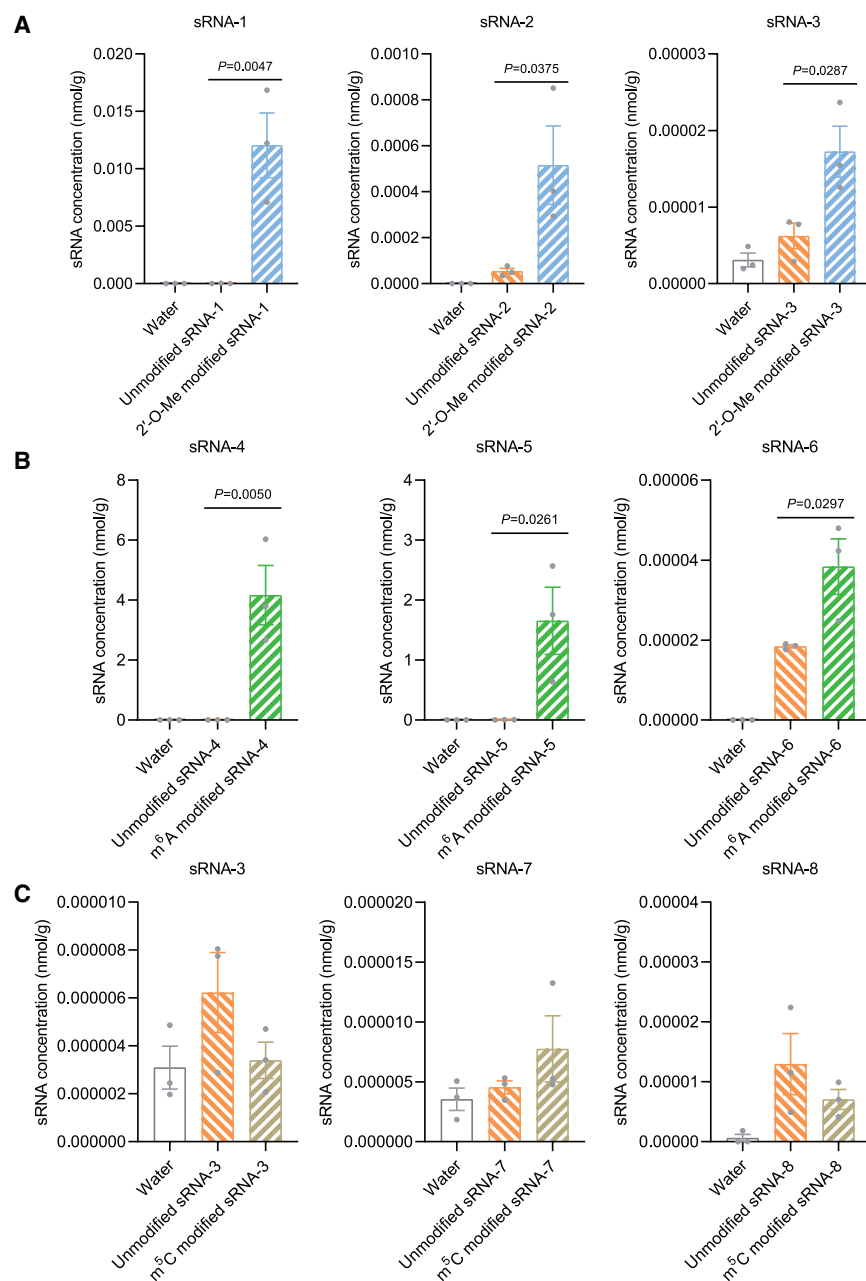


Figure 2. 2'-O-Me and m⁶A modification enhances the gastric uptake of small RNAs in pyloric-ligated mice

Bar graphs comparing the concentration of small RNA in the stomachs of pyloric-ligated mice after gavage feeding of unmodified small RNAs and RNAs incorporated with full-length 2'-O-Me (A), m⁶A (B), and m⁵C (C). The modification sites are detailed in Figure S4. Data represent mean \pm SEM, $n = 3$ independent experiments. Data were analyzed by one-way ANOVA with Tukey's multiple comparisons test.

sequences from Bencao (herbal) small RNA Atlas (<http://bencao.bmicc.cn>) were synthesized with these RNA modifications for further study.⁵ The modification sites are detailed in Figure S4.

2'-O-Me and m⁶A increase gastric absorption of small RNAs in pylorus-ligated mice

The stomach is pivotal in the digestive system, serving as a site for food storage and the initial absorption of nutrients. To assess the impact of RNA modifications on RNA uptake in the stomach, we evaluated the gastric absorption of small RNA in pylorus-ligated mice. After gavage feeding with unmodified or modified small RNA, the stomachs were collected, and the mucus layer was removed through thorough washing. Then stomach tissue was weighed and homogenized for RNA extraction. The quantity of small RNA was detected by stem-loop RT-qPCR, which has high specificity for detecting intact RNA. Both modified and unmodified small RNAs were absorbed to varying degrees in the stomachs of the mice after gavage. Notably, for sRNA-1, sRNA-2, and sRNA-3, 2'-O-Me significantly enhanced their gastric absorption in the pyloric ligation model (Figure 2A). Similarly, m⁶A also markedly increased the concentration of small RNAs in the stomach

four nucleotides.^{34,35} The relative contents of Am, Cm, Um, and Gm were 5.04%, 7.48%, 0.32%, and 0.12%, respectively, indicating that about 12.96% of nucleosides in BZL-derived small RNAs were modified with 2'-O-Me (Figure 1B). m⁶A, another prevalent RNA modification, exhibited 0.85% relative content in BZL-derived small RNAs (Figure 1B). Despite the abundance of 5-methylcytidine (m⁵C) in mRNA, its occurrence and function in microRNA are understudied.³⁶ Our finding of 8.61% m⁵C in herbal decoction-derived small RNA was notable (Figure 1B). In summary, 2'-O-Me, m⁶A, and m⁵C are prevalent in small RNAs from TCM decoction, with their impact on the oral delivery of small RNA yet unknown. To address this, several RNA

(Figure 2B). However, m⁵C did not demonstrate a promoting effect on gastric absorption (Figure 2C). Similar effect was observed in the uptake of adenocarcinoma gastric stomach (AGS) cells (Figure S5). We also measured the plasma concentration of small RNAs in both pyloric-ligated and sham-operated mice. The comparable plasma level of modified sRNA in both groups suggests that the stomach serves as the primary site for oral absorption of small RNAs, with the intestine playing a limited role in this process (Figure S6). This finding is consistent with a previous study on the absorption mechanism of dietary microRNAs.¹

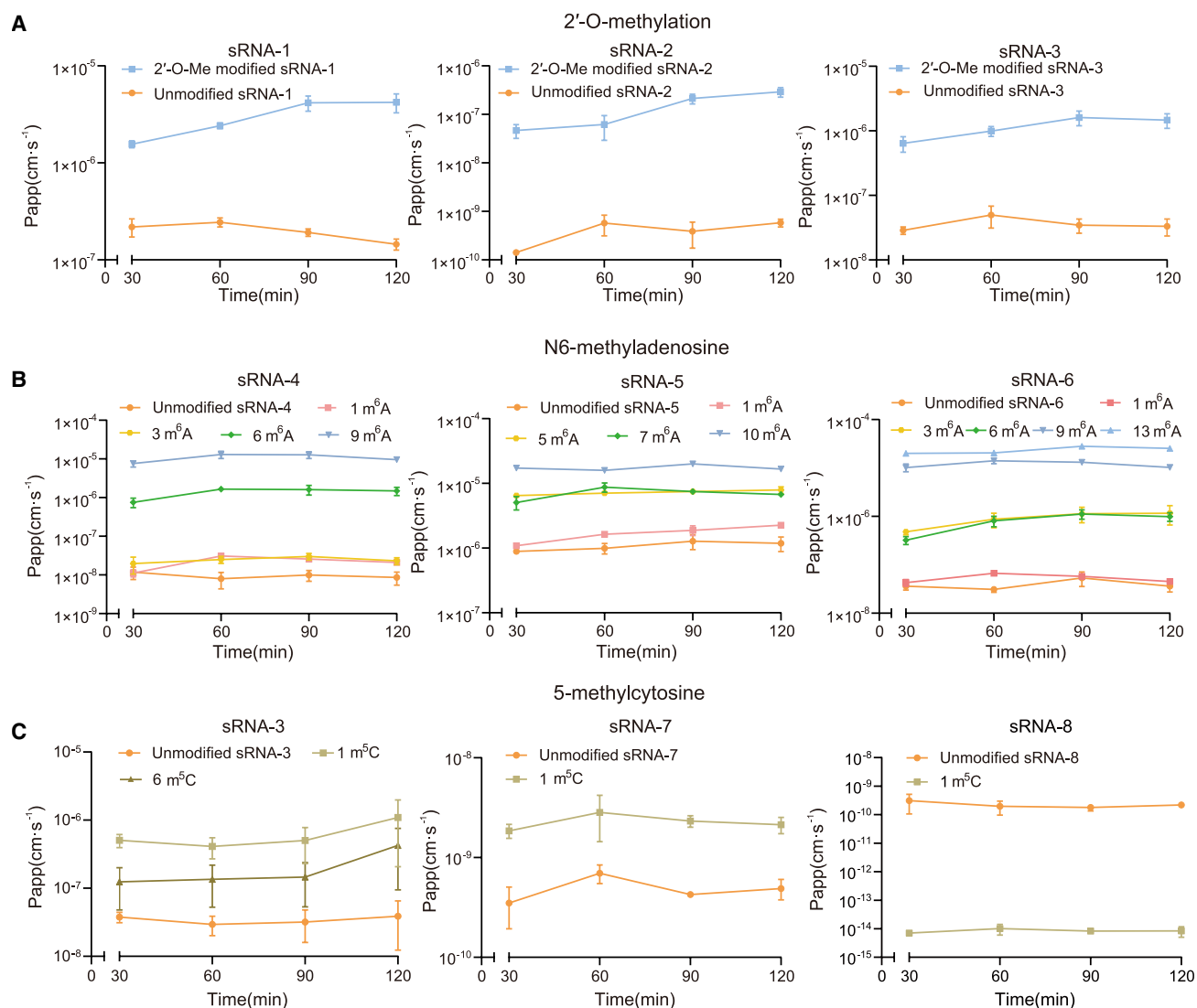


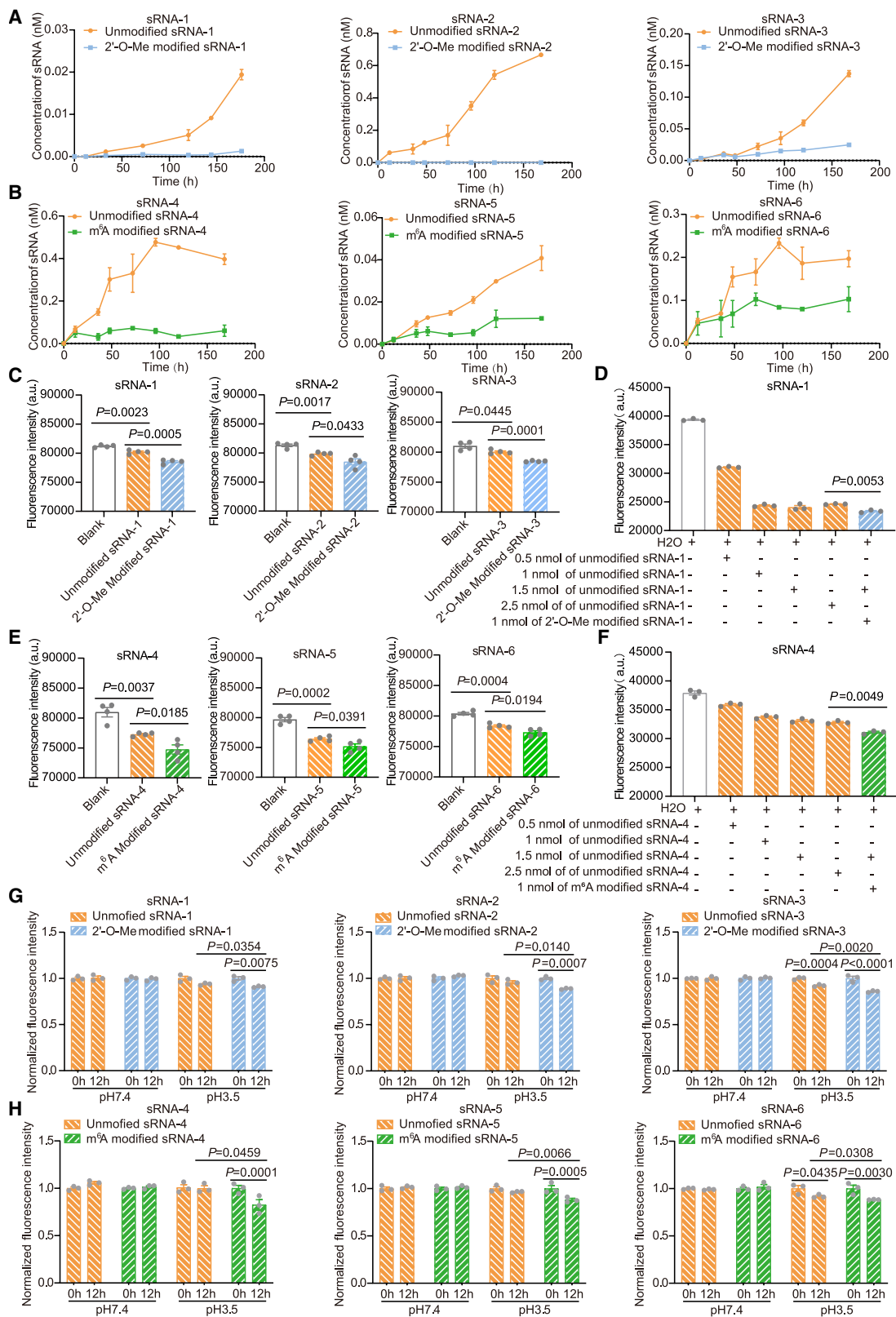
Figure 3. 2'-O-Me and m⁶A modification increases the permeability of small RNAs in Caco-2 monolayer

(A and C) Permeability assessment of RNAs modified with full-length 2'-O-Me or m⁵C in the Caco-2 monolayer at 30 min, 60 min, 90 min, and 120 min. (B) Determination of the apparent permeability coefficient of small RNA with varying amounts of m⁶A modification at 30 min, 60 min, 90 min, and 120 min. The modification sites are detailed in Figure S4. Papp, apparent permeability coefficient. Data represent mean \pm SEM, $n = 3$ independent experiments.

2'-O-Me and m⁶A increase permeability of sRNA in Caco-2 monolayer

Despite the intestine's limited role in direct oral RNA uptake, we evaluated the impact of chemical modifications on sRNA permeability across intestinal barriers. The Caco-2 monolayer cell model, which reconstructs human intestinal epithelial cells *in vitro*, is recognized as the gold standard by the Food and Drug Administration (FDA) for predicting drug absorption in the human intestine.³⁷ It is widely used for *in vitro* assessments of drug permeability and absorption.^{38–41} The apparent permeability coefficient (Papp) serves as a crucial metric, with values below 1.0×10^{-6} $\text{cm}\cdot\text{s}^{-1}$ indicating poor absorption, 1.0×10^{-6} $\text{cm}\cdot\text{s}^{-1}$ to 1.0×10^{-5} $\text{cm}\cdot\text{s}^{-1}$ suggesting mod-

erate absorption, and values exceeding 1.0×10^{-5} $\text{cm}\cdot\text{s}^{-1}$ signifying good absorption. In this study, we constructed a Caco-2 monolayer cell model to evaluate the permeability of small RNA (Figure S1B). The Papp values of all unmodified small RNAs were below 1.0×10^{-6} $\text{cm}\cdot\text{s}^{-1}$, indicating poor absorption in the Caco-2 monolayer cell model (Figures 3A–3C). However, full-length 2'-O-Me markedly increased the permeability of sRNA-1, sRNA-2, and sRNA-3 by 29-fold, 1087-fold, and 44-fold, respectively, reaching levels of moderate absorption (Figure 3A). Concerning m⁶A, the incorporation of one m⁶A to sRNA-4, sRNA-5, and sRNA-6 showed minimal improvement in Papp (Figure 3B). However, as the number of m⁶A increased, permeability improved in a quantity-dependent



(legend on next page)

manner, exceeding the good absorption level when nine or more adenosines were replaced by m⁶A (Figure 3B). The Log₁₀ value of Papp showed a positive relationship with the number of m⁶A, with Pearson coefficients for sRNA-4, sRNA-5, and sRNA-6 being 0.9756 ($p = 0.0046$), 0.9618 ($p = 0.0089$), and 0.9650 ($p = 0.0018$), respectively (Figure S7). In contrast, m⁵C did not consistently enhance small RNAs permeability (Figure 3C). These findings underscore the challenge unmodified small RNAs face in crossing the Caco-2 monolayer, whereas 2'-O-Me and m⁶A significantly improve their otherwise poor absorption, reaching levels of moderate and good absorption. We did not observe obvious changes in transepithelial electrical resistance (TEER) values after treating with small RNA in this study, suggesting that tight junction and monolayer integrity were not disrupted (Figure S8). Since no decrease in TEER was observed during treatment, it can be inferred that RNA is likely not absorbed via the paracellular pathway. (Figure S9). Additionally, as SIDT1 is limited to the stomach, RNA is unlikely to be transported via SIDT1 in the Caco-2 monolayer model. Previous studies have shown that oligonucleotides are typically absorbed through endocytosis.^{42,43} Therefore, we hypothesize that RNA is primarily absorbed via endocytosis in the Caco-2 monolayer model.

2'-O-Me and m⁶A promote the interaction between small RNAs and liposomes

A study on the oral delivery of GalNAc-conjugated siRNA indicates that the primary challenge for this delivery method lies not in stability but rather in permeability.¹⁸ Previous reports indicate that RNA can bind to phospholipid membranes through electrostatic and hydrophobic interactions, affecting membrane permeability.^{28,30,31} To investigate this interaction independently of RNA stability and protein interactions, we utilized DPPE-DSPE-PEG2000 10% cholesterol liposomes as a model of negatively charged cell membranes. The liposomes exhibited an average size of 138.9 nm, with a zeta potential of -42.59 ± 1.09 mV (Figure S10), providing an appropriate platform for studying the interaction. The experimental workflow was depicted in Figure S1C. Fewer 2'-O-Me- and m⁶A-modified small RNAs escaped from the dialysis tube, indicating that 2'-O-Me and m⁶A enhanced the interaction between RNA and liposomes (Figures 4A and 4B).

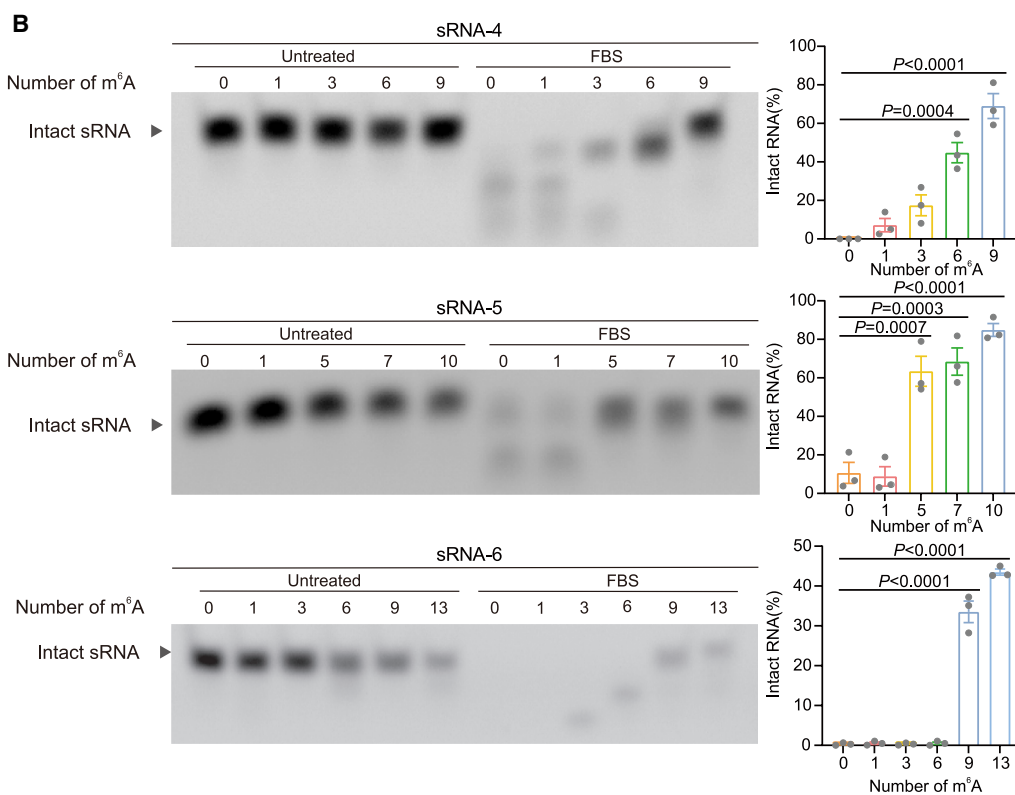
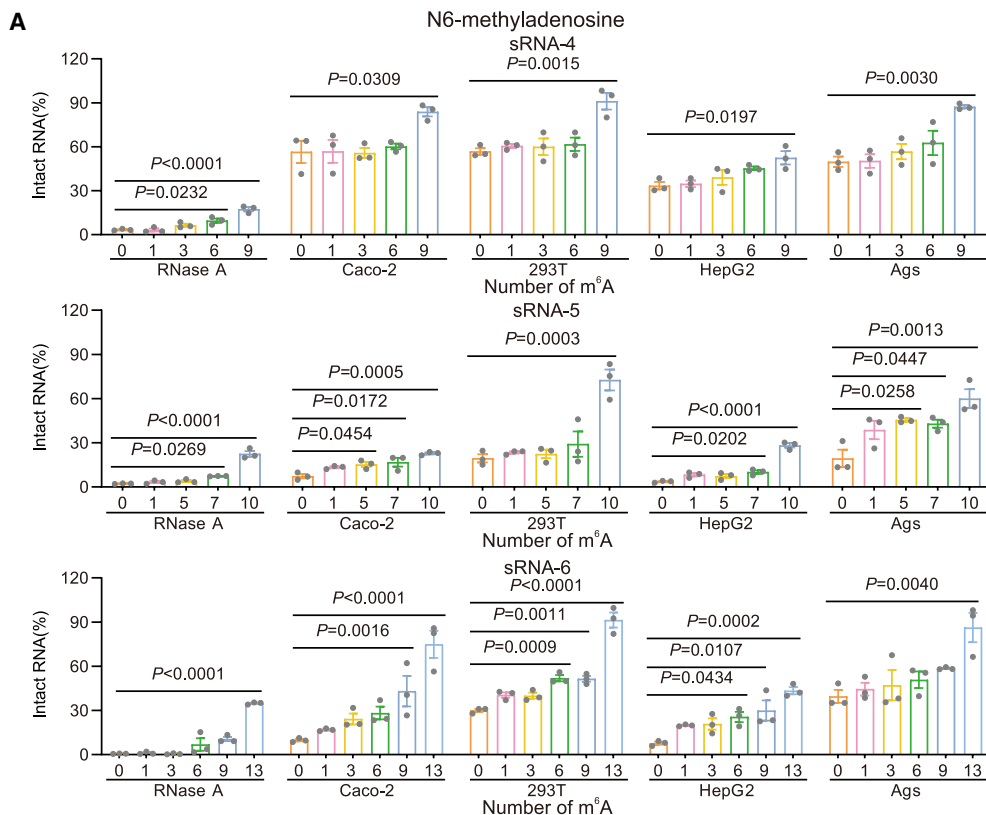
For further investigation, we assessed the interaction between liposomes and RNAs using a hydrophobic fluorescent probe, 6-(p-toluidino) naphthalene-2-sulfonate (TNS) (Figure S1D). TNS's fluo-

rescence intensity and its emission shift significantly depend on the polarity of the surrounding environment.^{30,44} The presence of RNA increased the Kd value of TNS with liposomes (Figure S11A). As the amount of small RNA added into the TNS-liposome system increased, the fluorescence intensity initially decreased and reached a plateau (Figures S11B–S11D). As there is no peak shift at different RNA concentrations, the decreased fluorescence intensity is attributed to the replacement of TNS by RNA, indicating interaction between RNA and liposomes.³⁰ Whether co-incubated with modified or unmodified small RNAs, the fluorescence intensity of the TNS-liposome mixture decreased, with 2'-O-Me- and m⁶A-modified small RNAs showing lower intensity than their unmodified counterparts (Figures 4C–4E). This indicates that a greater number of TNS molecules inserted into the liposomes were replaced. In a replacement assay, we monitored the changes in fluorescence intensity after introducing different amounts of unmodified small RNA. The fluorescence intensity initially decreased and reached a plateau when the amount reached 1.5 nmol. We further added 1 nmol of unmodified or modified small RNA into the mixture. We found that the fluorescence intensity was comparable between the 2.5 nmol unmodified sRNA group and the 1.5 nmol unmodified sRNA group. However, the addition of 1 nmol of 2'-O-Me-modified sRNA-1 or m⁶A-modified sRNA-4 further decreased the fluorescence intensity, indicating that these modifications enhance the affinity of small RNAs for liposomes (Figures 4D–4F). In contrast, the m⁵C modification did not exhibit a similar effect (Figure S11E). In summary, both 2'-O-Me and m⁶A enhance the RNA-lipid interaction.

To determine whether small RNAs only bound to the surface of liposomes or entered into the liposomal interior, extracellular RNAs were detected after mixing of small RNAs and liposomes (Figure S1E). The fluorescence intensity remained consistent at pH 7.4 for modified and unmodified small RNAs, indicating that small RNAs adhered exclusively to the surface of liposomes in a neutral environment. Unexpectedly, under low pH conditions, unmodified sRNA exhibited a slight reduction in fluorescence intensity after incubation with liposomes at pH 3.5, with 2'-O-Me- and m⁶A-modified small RNAs exhibiting lower fluorescence intensity compared to their unmodified counterparts (Figures 4G and 4H). The fluorescence intensity returned upon the addition of Triton (Figures S12A and S12B). These results indicate that 2'-O-Me and m⁶A promoted RNA traversal of lipid bilayers in an acidic environment. m⁵C modification did not demonstrate improvement in the permeability of small RNA (Figure S12C).

Figure 4. 2'-O-Me and m⁶A modification promotes the interaction between small RNAs and liposomes

(A and B) Concentration of full-length 2'-O-Me or m⁶A-modified RNAs, as well as their unmodified counterparts, in the external solution of the dialysis tube at 24 h, 48 h, 72 h, 96 h, 120 h, and 144 h. Absolute quantification of small RNA was performed using the standard curve method. Data represent mean \pm SEM, $n = 2$ independent experiments. (C and E) Bar graphs comparing the fluorescence intensity ($\lambda_{ex} = 360$ nm, $\lambda_{em} = 460$ nm) of full-length 2'-O-Me or m⁶A-modified RNAs (1 μ M) with their unmodified counterparts after a 1-h incubation with TNS-inserted liposomes at 37°C. Data represent mean \pm SEM, $n = 4$ independent experiments. (D and F) The change of fluorescence intensity after introducing 2'-O-Me-modified sRNA-1 or m⁶A-modified sRNA-4 to the TNS-liposome mixture whose fluorescence intensity had reached a plateau by gradually adding their unmodified counterparts to 1.5 nmol. (G and H) Full-length 2'-O-Me or m⁶A-modified RNAs were incubated with liposomes under pH 7.4 and pH 3.5 conditions. External small RNAs were detected with Quant-iT RiboGreen RNA Kit. Normalized fluorescence intensity compared to 0 h is calculated. The modification sites are detailed in Figure S4. Data represent mean \pm SEM, $n = 3$ independent experiments. Data were analyzed by Student's *t* test (two-tailed).



(legend on next page)

m⁶A improves small RNA biological stability

Previous studies have demonstrated the role of 2'-O-Me in enhancing the thermostability and biological stability of microRNA, as well as its efficacy in improving the bioavailability of antisense oligonucleotide (ASO) drugs.^{17,45} Regarding m⁶A, several studies have reported that while double-stranded RNA with m⁶A exhibits lower thermodynamic stability, it enhances the stability of unpaired positions near duplexes and encourages the adoption of a single-stranded structure in nucleotides upstream of the m⁶A site.^{46,47} To assess the stability of m⁶A-modified single-stranded small RNAs, sRNA-4, sRNA-5, and sRNA-6 incorporated with varying amounts of m⁶A underwent hydrolysis by endogenous nucleases in cell lysates and RNase A. The percentage of residual RNA of these small RNAs increased in a quantity-dependent manner (Figure 5A). We also conducted stability analysis in fetal bovine serum (FBS) (Figure S1F). Intact unmodified small RNAs were negligible after 0.5%FBS treatment, whereas increased intact RNA (%) was observed in modified sRNA-4, sRNA-5, and sRNA-6 as the number of m⁶A sites increased (Figure 5B). Enhanced stability of m⁶A-modified small RNAs was also observed in the stability assay with 10%FBS (Figure S13).

It is reported that m⁵C can be recognized and bound by Y-box binding protein 1 (YBX1), which preserves the stability of m⁵C-modified mRNA.^{48–50} However, in this study for small RNAs, m⁵C-modified small RNAs showed a comparable residual RNA level to their unmodified counterparts (Figure S14).

2'-O-Me and m⁶A enhance the oral delivery in mice

To investigate the effect of these RNA modifications on the oral delivery of plant-derived small RNAs in mice, the stability of modified small RNA in simulated gastric and intestinal fluids was assessed (Figure S15). Both modified and unmodified small RNAs were stable in simulated gastric fluid (Figure S15A). In simulated intestinal fluid, however, unmodified sRNA was almost completely degraded after 2 h, whereas 2'-O-Me- and m⁶A-modified small RNA showed enhanced stability compared to their unmodified counterparts. No such effect was observed for m⁵C (Figure S15B).

In the biodistribution study, unmodified and modified small RNAs were administered to mice via gavage feeding. At 3 h post-oral administration, 2'-O-Me-modified sRNA-1 and m⁶A-modified sRNA-5 showed markedly elevated levels in plasma and various organs compared to their unmodified counterparts (Figures 6A and 6B). In contrast, m⁵C did not demonstrate enhancement in the oral uptake of small RNA (Figure 6C). The oral bioavailability of unmodified sRNA-1 and sRNA-5 was 0.0087% and 0.0096%, respec-

tively, indicating that unmodified small RNAs are poorly absorbed into the systemic circulation when administered orally, whereas the bioavailability of 2'-O-Me-modified sRNA-1 and m⁶A-modified sRNA-5 was 2.88% and 3.01%, respectively (Figures 6D and 6E). These results suggest that these two modifications enable more efficient absorption of small RNAs from the gastrointestinal tract into the systemic circulation. The bioavailability of unmodified sRNA-3 and m⁵C-modified sRNA-3 was comparable, measuring 0.17% and 0.11%, respectively (Figure 6F). This suggests that the m⁵C modification does not enhance the absorption of sRNA into the systemic circulation. Unmodified sRNA-3 exhibited relatively higher bioavailability compared to sRNA-1 and sRNA-5. This may be attributed to its greater instability, which results in a smaller area under the curve (AUC) following intravenous injection.

DISCUSSION

The study focuses on understanding the mechanism of oral absorption of plant-derived small RNAs. We detect abundant 2'-O-Me, m⁶A, and m⁵C in BZL decoction small RNAs and discover that 2'-O-Me and m⁶A improve the oral delivery of plant-derived small RNAs both *in vitro* and *in vivo* by enhancing RNA stability and RNA-biomembrane interaction, whereas m⁵C does not demonstrate similar enhancement.

Previous investigations found that orally administered microRNAs were primarily absorbed in the stomach by SID-1 transmembrane family member 1 (SIDT1).^{1,51} Additionally, large-scale plant-derived small RNAs were identified in human blood samples from individuals who had consumed TCM decoctions.² After gavage feeding, orally administered microRNAs were detected in plasma, liver, lung, heart, and kidney.¹ These findings prompt inquiries into how these small RNAs bind to the cell membrane during stomach churning and remain intact during distribution to the blood or other organs, despite their hydrophilic and unstable nature. In this study, we discover that, in addition to improving RNA stability, 2'-O-Me and m⁶A also enhance the interaction between RNA and liposomes, as evidenced by less escape from the dialysis tube and lower fluorescence intensity in the TNS experiment (Figures 4A–4F). This enhancement might be attributed to the increased adherence of 2'-O-Me- and m⁶A-modified RNA to liposomes since small RNAs did not enter liposomes in a neutral environment (Figures 4G and 4H). Notably, small RNAs have entry under low pH conditions, particularly with 2'-O-Me and m⁶A promoting RNA entry into liposomes at pH 3.5.

Former studies on RNA-lipid interaction suggested that these interactions were driven by both electrostatic (phosphate backbone of

Figure 5. m⁶A modification increases the biological stability of small RNAs

(A) Residual (%) of small RNAs with varying amounts of m⁶A modifications after incubation with 0.1 U/μL RNase A, Caco-2 cell lysates, AGS cell lysates, HepG2 cell lysates, and 293T cell lysates for 15 min. The absolute quantification of small RNA was conducted using the standard curve method. Data represent mean ± SEM, *n* = 3 independent experiments. Data were analyzed by one-way ANOVA with Tukey's multiple comparisons test. (B) Representative PAGE gel showing the degradation of small RNA with varying amounts of m⁶A modifications after treatment with 0.5% FBS at 37°C for 15 min. The bands of RNAs without incubation with FBS were positioned on the left side of the image. Intact small RNAs were indicated by triangles. The modification sites are detailed in Figure S4. Data represent mean ± SEM, *n* = 3 independent experiments. Data were analyzed by one-way ANOVA with Tukey's multiple comparisons test. The uncropped gel image is provided in Figure S17–19.

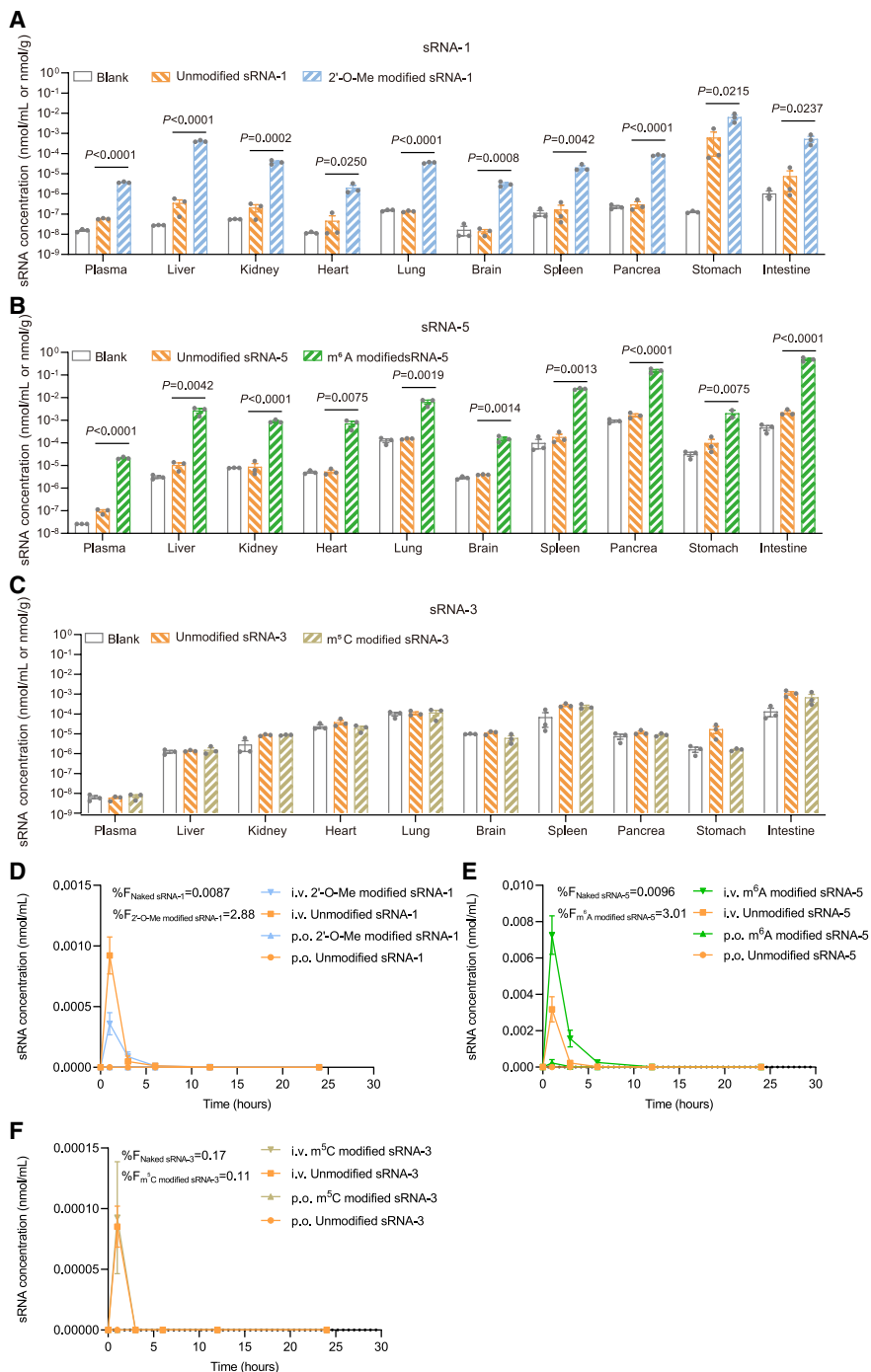


Figure 6. 2'-O-Me and m⁶A modification enhance the oral delivery of small RNAs in mice

Bar graph comparing the concentration of small RNAs in plasma and various organs of mice at 3 h after gavage feeding of 400 nmol/kg of 2'-OME-modified sRNA-1 (A), m⁶A-modified sRNA-5 (B), and m⁵C-modified sRNA-3 (C), along with their unmodified counterparts. The plasma concentration-time profiles following gavage or intravenous injection of 2'-O-Me-modified sRNA-1 (D), m⁶A-modified sRNA-5 (E), and m⁵C-modified sRNA-3 (F) are shown. The modification sites are detailed in Figure S4. Data represent mean ± SEM, n = 3 independent experiments. Data were analyzed by unpaired Student's t test(two-tailed).

Table 1. The sequence of small RNAs used in this experiment

No.	Sequence
sRNA-1	GUUCAGAGUUCUACAGUCCGACGA
sRNA-2	GAUGGAUUUGAGUAAGAGCGUAG
sRNA-3	AGCUGGAAACGGCUGCUAAUACC
sRNA-4	ACCAAAGCUAGCUACAUA
sRNA-5	UAUAGGGGCGAAAAGACUAAUCGAA
sRNA-6	ACAAAAGCAAAACAGGUCUAGAA
sRNA-7	GGAAUGUAAAGAAGUAUGUAC
sRNA-8	UGGAAUGUAAAGAAGUAUGUAC

RNA and lipid head) and hydrophobic forces (nucleobase and lipid tail).^{30,31} Methylation increases the hydrophobicity of oligonucleotides.⁵² In this study, 2'-O-Me and m⁶A may strengthen the hydrophobic interaction between RNA and liposomes. The mechanism underlying small RNA entry into liposomes at pH 3.5, with enhanced entry by 2'-O-Me and m⁶A, requires further investigation.

RNA-based therapeutics, such as mRNA vaccines and oligonucleotide drugs, are gaining prominence for simplifying drug target identification compared to conventional chemical compounds and protein-based drugs.^{45,53} In FDA-approved nucleic acid-based therapeutics, chemical modifications like phosphorothioates, 2'-O-Me, 2'-fluoro (2'-F), 2'-O-methoxyethylation (2'-MOE), and phosphorodiamidate morpholino oligomers (PMOs) are incorporated to enhance metabolic stability.^{12,54} Notably, lipid nanoparticle (LNP) delivery systems and GalNAc conjugation greatly improve oligonucleotide delivery efficiency.^{12,55} Oral administration of nucleic acids offers advantages such as patient compliance, cost-effectiveness, and potential therapeutic benefits for gastrointestinal disorders, prompting research into effective oral delivery strategies.⁵⁶ Several studies have explored the potential for developing oral oligonucleotide therapeutics.^{19–21} Our experiment observed enhanced oral delivery of plant-derived small RNAs incorporated with 2'-O-Me and m⁶A both *in vitro* and *in vivo*. Future development of orally administered oligonucleotides could explore the application of 2'-O-Me and m⁶A.

In conclusion, our study emphasizes the role of 2'-O-Me and m⁶A in enhancing small RNA oral delivery by facilitating RNA-bio-membrane interaction and improving biological stability, providing insights for nucleic acid oral delivery strategies.

MATERIALS AND METHODS

Cell cultures

HepG2, HEK293T, AGS, and Caco-2 cells were all acquired from the Peking Union Medical College Cell Culture Center. HEK293T and HepG2 cells were grown in DMEM. AGS cells were grown in RPMI-1640 medium. RPMI-1640 medium and DMEM were supplemented with 10% fetal bovine serum (FBS, Hyclone) and 1% 100 × Penicillin-Streptomycin (Gibco). Caco-2 cells were cultured

in minimum essential medium (MEM) with 20% FBS. Cells were maintained at 37°C with 5% CO₂.

RNA sequences

All RNAs were synthesized by Sangon Biotech (China). RNA sequences are provided in Table 1.

CTAB lysis buffer preparation

CTAB lysis buffer was prepared by dissolving 7.2 g of ethylenediaminetetraacetic acid (EDTA, Sinopharm Chemical Reagent, China), 20 g of hexadecyltrimethylammonium bromide (CTAB, AMRESCO), 20 g of polyvinylpyrrolidone-40 (PVP-40, Lablead), 117 g of NaCl (Solarbio), 0.5 g of spermidine (Sigma-Aldrich), and 12 g of Tris (AMRESCO) in 960 mL of DEPC-treated deionized water. Add 1 mL of DEPC (Sigma-Aldrich) to the solution and stir overnight. The solution was adjusted to pH 8.0 and diluted to 1L with DEPC-treated deionized water. DEPC was deactivated by a high-pressure, high-temperature process; 2% thioglycol was added before use.

Small RNA extraction of TCM decoction

Ban Zhi Lian (*Scutellaria barbata*), a traditional Chinese medicine, was purchased from TongRenTang pharmacy (Beijing, China). The preparation of the decoction of BZL and RNA extraction of the decoction were performed as previously described.⁵ Tissue miRNA Kit (Vazyme, China) was used to exclude RNA sequences over 200 nt. Then the obtained RNA samples were resolved with 15% native polyacrylamide gel electrophoresis (PAGE). The area of 18–30 nt in the gels was collected and extracted by miRNA PAGE gel extraction kit (Anyang, China).

LC-MS-based RNA modifications detection

Qubit RNA HS Assay kit (Q32855, Thermo Fisher) was used to quantify RNA samples. These samples underwent hydrolysis and dephosphorylation into single nucleosides at 37°C for 3 h using an enzyme mix composed of 0.1 U phosphodiesterase I (UnitedStatesBiological), 10 U Benzonase (Sigma), and 1 U alkaline phosphatase (New England Biolabs). After ultrafiltration to remove proteins, the hydrolyzed RNA samples were injected into an LC-MS system. High-performance liquid chromatography (HPLC) conditions were established as Table S1. Solution A was 0.1% (v/v) formic acid. Solution B was prepared by mixing formic acid into pure acetonitrile, adjusting the concentration to 0.1% (v/v). The mass parameters were set up as Table S2.

The Agilent Qualitative Analysis software was used to extract peak data for modified nucleosides in the sample. Following this, peak areas were normalized according to the amount of injected small RNAs from the sample. The relative proportion (%) of modified nucleosides was determined by dividing the peak area of specific modified nucleosides by the total peak area.

Small RNA uptake assay in AGS cells

The pH of culture medium was adjusted to 3.5 using HCl; 2.5 μL of 20 μM small RNA were added to 500 μL culture medium. AGS cells

were exposed to small RNA (100 nM) in culture medium at 37°C for 30 min. After incubation, the cells were washed three times with PBS and treated with 0.1 U/mL RNase A for 30 min to digest extracellularly attached small RNAs. Total RNA was extracted with TRIzol reagent (Invitrogen). For the control group, AGS cells were exposed to blank culture medium, and the same amount of small RNAs was added to the sample after lysing with TRIzol reagent. For the negative control group in Figure S5D, the same amount of small RNAs were added to cells without incubation to represent the nonspecific binding RNAs. Real-time qPCR was performed to determine the relative RNA level compared to U6. The percentage of small RNA uptake was calculated using Equation 1.

$$\text{RNA uptake (\%)} = \left(2^{-(\Delta Ct \text{ of small RNA group})} / 2^{-(\Delta Ct \text{ of control group})} \right) \times 100 \quad (1)$$

Gastric absorption in pylorus-ligated mice

After a 12-h fasting period, six-week-old male C57BL/6 mice received pentobarbital sodium via intraperitoneal injection for anesthesia. Once the mice reached an adequate level of anesthesia, we performed the pyloric ligation surgery. After recovery, the mice were administered 200 μL of either unmodified or modified small RNA (400 nmol/kg) dissolved in RNase-free H_2O via gavage feeding. For the control group, the mice were administered 200 μL of RNase-free H_2O . Three hours later, we collected their stomachs for analysis. During the gastric lavage procedure, we made an incision along the greater curvature of the stomach, emptied the gastric contents, and carefully scraped off the mucus layer using a large volume of PBS. After thoroughly washing the stomach five times, we used filter paper to absorb any excess liquid from the tissue. The stomach tissue was then weighed and homogenized for RNA extraction.

RNA isolation and RT-qPCR of small RNAs

TRIzol reagent (Invitrogen) was used to extract total RNA from cells or tissues. Real-time quantification of small RNA was conducted using stem-loop RT-qPCR assays with High-Capacity cDNA Reverse Transcription Kit (Applied Biosystems), LightCycler 480 SYBR Green I Master Kit, and LightCycler 480 PCR System (Roche). For absolute quantification, recognizing that modifications may influence primer binding or the affinity of small RNA to reverse transcriptase, an absolute quantification method was employed. The RNA concentration of unknown samples was calculated by comparing their Ct values to those on the standard curve (Figure S16). A standard curve was established by correlating the logarithm of small RNA concentration with Ct values through linear regression analysis. The concentration of unknown RNA samples was determined by comparing their Ct values to the standard curve. For relative quantification, the Delta-C_t method was used to calculate the relative RNA level compared to U6. The primer sequences are provided in Table S3.

Caco-2 monolayer model

Two hundred microliters of MEM was added to pre-wet the apical side of transwells for at least 2 min. The MEM was replaced with

500 μL of Caco-2 cell suspension (2×10^5 cells/mL). The basolateral chamber was filled with 1.5 mL of MEM. The transwells were then incubated in a 37°C incubator with 5% CO_2 for 12 h. Replace the culture medium with fresh MEM. The cells were maintained by replacing all culture medium every second day for a total of 21 days. By day 21, quality control experiments for the Caco-2 monolayer model were conducted. The transepithelial electrical resistance (TEER) value at 37°C was measured using an RE1600 transmembrane cell resistance meter (Beijing Jinggong Hongtai Technology, China). Lucifer yellow permeability was evaluated as an indicator of monolayer integrity. The Caco-2 monolayer model was considered successful only when the TEER was greater than $500 \Omega \text{ cm}^{-2}$ and the Papp of lucifer yellow was below $0.5 \times 10^{-6} \text{ cm s}^{-1}$.

Determination of the permeability of small RNA

The Hank's balanced salt solution (HBSS) was preheated to 37°C. To determine the permeability of small RNA, the transwells were transferred to a new 12-well cluster and gently washed with HBSS to remove residual medium. Subsequently, add 500 μL and 1.5 mL of HBSS to the apical side and the basolateral side. The transwells were then incubated on an orbital shaker (100 rpm) for 20 min at 37°C. The solution in the apical compartment was replaced with 400 μL of small RNA solution (100 nM in HBSS), and the solution in the basolateral side was replaced with 1,200 μL of blank HBSS. The transwells were further incubated on an orbital shaker at 37°C. Half of the volume of the solution from the basolateral compartment was collected and supplemented with the same volume of blank HBSS at specified intervals (30, 60, 90, 120 min). Apparent permeability coefficient (Papp) is determined based on the amount of RNA transported at each time point. The Papp ($\text{cm} \cdot \text{s}^{-1}$) value is calculated according to Equation 2:

$$P_{app} = \left(\frac{\Delta Q}{\Delta t} \right) \times \left(\frac{1}{A \times C_0} \right) \quad (2)$$

where ΔQ is the amount of RNA transported across the Caco-2 monolayer (nmol), Δt is the time interval (s), A refers to the surface area of the transwell (cm^2), and C_0 refers to concentration of the initial small RNA solution (nM).

Dialysis of liposomes and small RNAs

The 50 kDa dialysis tube MD34 (Yeasen, China) was activated following the manufacturer's instructions and treated with 0.1% DEPC (Sigma-Aldrich, USA) overnight. After activation, the dialysis tubes were sterilized and stored in 20% ethanol. Two milliliters of liposomes (2.5 mg/mL) with 2 mL of small RNA (200 nM) were mixed together and incubated at 4°C for 12 h. The resulting mixture was then added to the dialysis tubes and dialyzed in 30 mL of RNase-free H_2O supplemented with RNase Inhibitor (Solarbio, China) and 1% $100 \times$ Penicillin-Streptomycin (Gibco) at 4°C. The dialysis apparatus was placed on an orbital shaker ($100 \text{ r} \cdot \text{min}^{-1}$). The concentrations of small RNA in the solution outside the dialysis tube at different time intervals were quantified.

Fluorescence measurement of TNS

The mixture of 50 μL of 40 μM TNS (Sigma-Aldrich) and 50 μL of liposomes (2.5 mg/mL) was incubated in the dark at 25°C for 1 h to facilitate TNS insertion. Five microliters of unmodified or modified small RNA solution (20 μM) was incorporated into the mixture, followed by incubation in the dark at 37°C for 1 h. In control group, sRNA was replaced by 5 μL RNase-free H_2O . The fluorescence intensity was measured with Biotek Synergy H1 Multimode Reader (Agilent, USA). In the fluorescence titration assay, 110 μL of liposome solution (2.5 mg/mL), 22 μL of TNS solution at varying concentrations, and 308 μL of RNase-free H_2O were mixed and incubated at 37°C for 1 h. Subsequently, 300 μL of the liposome-TNS solution was transferred into a new tube, and 15 μL of 20 μM RNA solution or 15 μL of RNase-free H_2O was added. The fluorescence intensity was then measured after further incubation at 37°C for 40 min. In the replacement assay, 22.5 μL of RNase-free H_2O or unmodified small RNA solution at varying concentrations was added into 300 μL of the liposome-TNS solution (containing 0.625 mg/mL liposomes and 5 μM TNS) and incubated at 37°C for 40 min. In the replacement group, 15 μL of 100 μM unmodified small RNA solution, 5 μL of 200 μM modified small RNA solution, and 2.5 μL of RNase-free H_2O were added. The fluorescence intensity was measured.

Detection of small RNAs outside the liposomes

Fifty microliters of liposomes (2.5 mg/mL) and 50 μL of small RNA (1 μM) were mixed together and incubated at 4°C for 12 and 0 h. Small RNA outside the liposomes was quantified with Quant-iT RiboGreen RNA Kit (Invitrogen). During the detection process, the TE buffer was replaced with a 2% Triton buffer in the corresponding groups in Figure S12.

Determining biostability of small RNAs

Protection of RNA from RNase A

A mixture of 10 μL of 200 nM small RNA solution and 90 μL of 0.1 U μL^{-1} RNase A were incubated at 37°C for 15 min. Transfer the mixture to liquid nitrogen to halt digestion. The residual small RNAs were quantified.

Protection of RNA from cell lysates

Caco-2, AGS, HEK293T, and HepG2 cells were resuspended in PBS and adjusted to 2×10^5 cells/mL. The cells were disrupted using a non-contact ultrasonic cell crusher Bioruptor Plus (Diagenode, Belgium) at 4°C with eight cycles (320 W, run 30s, pause 30s). Next, a mixture of 10 μL of 200 nM small RNA solution and 90 μL of cell lysates was incubated at 37°C for 15 min. Transfer the mixture to liquid nitrogen to halt digestion. The residual small RNAs were quantified.

Protection of RNA from FBS

In the stability assay of 0.5% FBS, a mixture of 10 μL of 20 μM small RNA solution and 10 μL of 1% FBS was incubated at 37°C for 15 min. In the stability assay of 10% FBS, 10 μL of 200 μM modified or unmodified sRNA was mixed with 10 μL of 20% FBS and incubated

at 37°C for 5 min. Subsequently, 4 μL of $6 \times$ RNA loading buffer for denaturing PAGE was added to the solution and boiled at 95°C for 2 min. We resolved the samples using 15% denaturing polyacrylamide gel electrophoresis (PAGE). After electrophoresis at 180 V for 50 min, the gels were transferred to 50 mL of 0.1 M NaCl solution containing $3 \times$ GelRed Nucleic Acid Stain (Lablead, China) for staining. The gels were visualized using the Tanon 1600 gel imaging system and processed using Gel-Pro Analyzer 4.0 software.

Biodistribution study of RNA

All experimental protocols involving animals were approved by the Institutional Animal Care and Use Committee. Intragastric administration of 400 nmol/kg body weight of unmodified or modified small RNAs was performed on 9-week-old C57BL/6 mice. Plasma and various organs were collected 3 h after gavage feeding of small RNAs. The organ samples were cleared of content by washing with PBS three times. The weight of different organ samples was measured after blotting with filter papers. Total RNA of plasma and organ samples was extracted. Absolute quantification of small RNA was conducted.

Bioavailability study of RNA

Eight-week-old male C57BL/6 mice received 400 nmol/kg body weight of either unmodified or modified small RNAs via gavage or tail vein injection. Collect blood samples at 1, 3, 6, 12, and 24 h post-administration. Total RNA from plasma and organ samples was isolated. Absolute quantification of small RNA was conducted. Oral bioavailability relative to i.v. dose was calculated according to Equation 3:

$$\text{Bioavailability (\%F)} = \left(\text{AUC}_{i.g.} \times \text{Dose}_{i.v.} \right) / \left(\text{AUC}_{i.v.} \times \text{Dose}_{i.g.} \right) \times 100 \quad (3)$$

Statistical analysis

Statistical tests were performed using GraphPad Prism 9.

DATA AVAILABILITY

All data are incorporated into the article and its supplemental information.

ACKNOWLEDGMENTS

This work was supported by the National Natural Science Foundation of China (81788101), Chinese Academy of Medical Sciences Innovation Fund for Medical Sciences (2021-I2M-1-022, 2022-I2M-CoV19-001), 111 Project (BP0820029), the CAMS Endowment Fund (2021-CAMS-JZ001), State Key Laboratory Special Fund (2060204), and Fundamental Research Funds for Central Universities (2017PT31017).

We acknowledge the use of ChatGPT 3.5 (<https://chat.openai.com/>), an artificial intelligence language model developed by OpenAI, for English editing of this manuscript.

The graphics in Figure S1 and graphical abstract were created with BioRender.com.

AUTHOR CONTRIBUTIONS

C.J. designed this study and supervised the experimental work. C.J. and S.G. wrote the manuscript. S.G. and Z.Li. performed the detection of RNA modifications. S.G. and Z.Li. carried out and analyzed the uptake of sRNA in AGS cells. S.G., Z.Li., and X.L.

constructed the Caco-2 monolayer model and determined the permeability of sRNA. S. G., Z.Li., and X.L. conducted experiments on RNA stability. S.G., Z.Li., and X.L. conducted experiments on the interaction between RNA and liposomes. S.G. and Z.Li. performed *in vivo* experiments of sRNA oral delivery. Z.Liang, D.Z., N.S., J.L., X.W., S.M., and X.Q. contributed to the exploration of preliminary experiments.

DECLARATION OF INTERESTS

The authors declare no competing interests.

DECLARATION OF GENERATIVE AI AND AI-ASSISTED TECHNOLOGIES IN THE WRITING PROCESS

During the preparation of this work, the author(s) used ChatGPT 3.5 (<https://chat.openai.com/>) in order to check grammar errors. After using this tool/service, the author(s) reviewed and edited the content as needed and take(s) full responsibility for the content of the publication.

SUPPLEMENTAL INFORMATION

Supplemental information can be found online at <https://doi.org/10.1016/j.omtn.2025.102574>.

REFERENCES

- Chen, Q., Zhang, F., Dong, L., Wu, H., Xu, J., Li, H., Wang, J., Zhou, Z., Liu, C., Wang, Y., et al. (2021). SIDT1-dependent absorption in the stomach mediates host uptake of dietary and orally administered microRNAs. *Cell Res.* *31*, 247–258.
- Huang, F., Du, J., Liang, Z., Xu, Z., Xu, J., Zhao, Y., Lin, Y., Mei, S., He, Q., Zhu, J., et al. (2019). Large-scale analysis of small RNAs derived from traditional Chinese herbs in human tissues. *Sci. China Life Sci.* *62*, 321–332.
- Liang, G., Zhu, Y., Sun, B., Shao, Y., Jing, A., Wang, J., and Xiao, Z. (2014). Assessing the survival of exogenous plant microRNA in mice. *Food Sci. Nutr.* *2*, 380–388.
- Liang, H., Zhang, S., Fu, Z., Wang, Y., Wang, N., Liu, Y., Zhao, C., Wu, J., Hu, Y., Zhang, J., et al. (2015). Effective detection and quantification of dietetically absorbed plant microRNAs in human plasma. *J. Nutr. Biochem.* *26*, 505–512.
- Cao, Y., Lin, Y., Sun, N., Du, X., Dong, Y., Mei, S., Deng, X., Li, X., Guo, S., Tang, K., et al. (2023). A comprehensive analysis of the Bencao (herbal) small RNA Atlas reveals novel RNA therapeutics for treating human diseases. *Sci. China Life Sci.* *66*, 2380–2398.
- Tang, K., Wang, X., Zhao, Y., Li, X., Jiang, Z., Mei, S., Chen, M., Ma, Y., Du, X., Qiao, X., et al. (2023). Oral administration of the herbal oligonucleotide XKC-sRNA-h3 prevents angiotensin II-induced hypertension in mice. *Sci. China Life Sci.* *66*, 2370–2379.
- Li, X., Liang, Z., Du, J., Wang, Z., Mei, S., Li, Z., Zhao, Y., Zhao, D., Ma, Y., Ye, J., et al. (2019). Herbal decoctosome is a novel form of medicine. *Sci. China Life Sci.* *62*, 333–348.
- Zhao, D., Qin, Y., Liu, J., Tang, K., Lu, S., Liu, Z., Lin, Y., Zhang, C., Huang, F., Chang, J., et al. (2023). Orally administered BZL-sRNA-20 oligonucleotide targeting TLR4 effectively ameliorates acute lung injury in mice. *Sci. China Life Sci.* *66*, 1589–1599.
- Zhou, Z., Li, X., Liu, J., Dong, L., Chen, Q., Liu, J., Kong, H., Zhang, Q., Qi, X., Hou, D., et al. (2015). Honeysuckle-encoded atypical microRNA2911 directly targets influenza A viruses. *Cell Res.* *25*, 39–49.
- Arevalo, C.P., Bolton, M.J., Le Sage, V., Ye, N., Furey, C., Muramatsu, H., Alameh, M.G., Pardi, N., Drapeau, E.M., Parkhouse, K., et al. (2022). A multivalent nucleoside-modified mRNA vaccine against all known influenza virus subtypes. *Science* *378*, 899–904.
- Chalkias, S., Harper, C., Vrbcicky, K., Walsh, S.R., Essink, B., Brosz, A., McGhee, N., Tomassini, J.E., Chen, X., Chang, Y., et al. (2022). A Bivalent Omicron-Containing Booster Vaccine against Covid-19. *N. Engl. J. Med.* *387*, 1279–1291.
- Egeli, M., and Manoharan, M. (2023). Chemistry, structure and function of approved oligonucleotide therapeutics. *Nucleic Acids Res.* *51*, 2529–2573.
- Boccaletto, P., Stefaniak, F., Ray, A., Cappannini, A., Mukherjee, S., Purta, E., Kurkowska, M., Shirvanizadeh, N., Destefanis, E., Groza, P., et al. (2022). MODOMICS: a database of RNA modification pathways. 2021 update. *Nucleic Acids Res.* *50*, D231–D235.
- Karikó, K., Muramatsu, H., Welsh, F.A., Ludwig, J., Kato, H., Akira, S., and Weissman, D. (2008). Incorporation of pseudouridine into mRNA yields superior nonimmunogenic vector with increased translational capacity and biological stability. *Mol. Ther.* *16*, 1833–1840.
- Yu, B., Yang, Z., Li, J., Minakhina, S., Yang, M., Padgett, R.W., Steward, R., and Chen, X. (2005). Methylation as a Crucial Step in Plant microRNA Biogenesis. *Science* *307*, 932–935.
- Abou Assi, H., Rangadurai, A.K., Shi, H., Liu, B., Clay, M.C., Erharter, K., Kreutz, C., Holley, C.L., and Al-Hashimi, H.M. (2020). 2'-O-Methylation can increase the abundance and lifetime of alternative RNA conformational states. *Nucleic Acids Res.* *48*, 12365–12379.
- Liang, H., Jiao, Z., Rong, W., Qu, S., Liao, Z., Sun, X., Wei, Y., Zhao, Q., Wang, J., Liu, Y., et al. (2020). 3'-Terminal 2'-O-methylation of lung cancer miR-21-5p enhances its stability and association with Argonaute 2. *Nucleic Acids Res.* *48*, 7027–7040.
- Yu, M., Qin, J., Liu, X., Ramsden, D., Williams, B., Zlatev, I., Guenther, D., Matsuda, S., Tymon, R., Darcy, J., et al. (2024). Evaluating the oral delivery of GalNAc-conjugated siRNAs in rodents and non-human primates. *Nucleic Acids Res.* *52*, 5423–5437.
- Tillman, L.G., Geary, R.S., and Hardee, G.E. (2008). Oral delivery of antisense oligonucleotides in man. *J. Pharm. Sci.* *97*, 225–236.
- Raouf, A.A., Chiu, P., Ramtoola, Z., Cumming, I.K., Teng, C., Weinbach, S.P., Hardee, G.E., Levin, A.A., and Geary, R.S. (2004). Oral bioavailability and multiple dose tolerability of an antisense oligonucleotide tablet formulated with sodium caprate. *J. Pharm. Sci.* *93*, 1431–1439.
- Gennemark, P., Walter, K., Clemmensen, N., Rekić, D., Nilsson, C.A.M., Knöchel, J., Hölttä, M., Wernevik, L., Rosengren, B., Kakol-Palm, D., et al. (2021). An oral antisense oligonucleotide for PCSK9 inhibition. *Sci. Transl. Med.* *13*, eabe9117.
- Crooke, S.T., Wang, S., Vickers, T.A., Shen, W., and Liang, X-h (2017). Cellular uptake and trafficking of antisense oligonucleotides. *Nat. Biotechnol.* *35*, 230–237.
- Wang, S., Allen, N., Vickers, T.A., Revenko, A.S., Sun, H., Liang, X.H., and Crooke, S.T. (2018). Cellular uptake mediated by epidermal growth factor receptor facilitates the intracellular activity of phosphorothioate-modified antisense oligonucleotides. *Nucleic Acids Res.* *46*, 3579–3594.
- Miller, C.M., Donner, A.J., Blank, E.E., Egger, A.W., Kellar, B.M., Østergaard, M.E., Seth, P.P., and Harris, E.N. (2016). Stabilin-1 and Stabilin-2 are specific receptors for the cellular internalization of phosphorothioate-modified antisense oligonucleotides (ASOs) in the liver. *Nucleic Acids Res.* *44*, 2782–2794.
- Cui, H., Zhu, X., Li, S., Wang, P., and Fang, J. (2021). Liver-Targeted Delivery of Oligonucleotides with N-Acetylgalactosamine Conjugation. *ACS Omega* *6*, 16259–16265.
- Prakash, T.P., Graham, M.J., Yu, J., Carty, R., Low, A., Chappell, A., Schmidt, K., Zhao, C., Aghajan, M., Murray, H.F., et al. (2014). Targeted delivery of antisense oligonucleotides to hepatocytes using triantennary N-acetyl galactosamine improves potency 10-fold in mice. *Nucleic Acids Res.* *42*, 8796–8807.
- Budker, V.G., Godovikov, A.A., Naumova, L.P., and Slepneva, I.A. (1980). Interaction of polynucleotides with natural and model membranes. *Nucleic Acids Res.* *8*, 2499–2515.
- Khvorova, A., Kwak, Y.G., Tamkun, M., Majerfeld, I., and Yarus, M. (1999). RNAs that bind and change the permeability of phospholipid membranes. *Proc. Natl. Acad. Sci. USA* *96*, 10649–10654.
- Vlassov, A., Khvorova, A., and Yarus, M. (2001). Binding and disruption of phospholipid bilayers by supramolecular RNA complexes. *Proc. Natl. Acad. Sci. USA* *98*, 7706–7711.
- Suga, K., Tanabe, T., Tomita, H., Shimanouchi, T., and Umakoshi, H. (2011). Conformational change of single-stranded RNAs induced by liposome binding. *Nucleic Acids Res.* *39*, 8891–8900.
- Marty, R., N'Soukpoé-Kossi, C.N., Charbonneau, D.M., Kreplak, L., and Tajmir-Riahi, H.A. (2009). Structural characterization of cationic lipid-tRNA complexes. *Nucleic Acids Res.* *37*, 5197–5207.

32. Czerniak, T., and Saenz, J.P. (2022). Lipid membranes modulate the activity of RNA through sequence-dependent interactions. *Proc. Natl. Acad. Sci. USA* *119*, e2119235119.
33. Wayment-Steele, H.K., Kim, D.S., Choe, C.A., Nicol, J.J., Wellington-Oguri, R., Watkins, A.M., Parra Sperberg, R.A., Huang, P.S., Participants, E., and Das, R. (2021). Theoretical basis for stabilizing messenger RNA through secondary structure design. *Nucleic Acids Res.* *49*, 10604–10617.
34. Elliott, B.A., Ho, H.T., Ranganathan, S.V., Vangaveti, S., Ilkayeva, O., Abou Assi, H., Choi, A.K., Agris, P.F., and Holley, C.L. (2019). Modification of messenger RNA by 2'-O-methylation regulates gene expression in vivo. *Nat. Commun.* *10*, 3401.
35. Marchand, V., Pichot, F., Thüring, K., Ayadi, L., Freund, I., Dalpke, A., Helm, M., and Motorin, Y. (2017). Next-Generation Sequencing-Based RiboMethSeq Protocol for Analysis of tRNA 2'-O-Methylation. *Biomolecules* *7*, 13.
36. Meyer, K.D., and Jaffrey, S.R. (2014). The dynamic epitranscriptome: N6-methyladenosine and gene expression control. *Nat. Rev. Mol. Cell Biol.* *15*, 313–326.
37. Hubatsch, I., Ragnarsson, E.G.E., and Artursson, P. (2007). Determination of drug permeability and prediction of drug absorption in Caco-2 monolayers. *Nat. Protoc.* *2*, 2111–2119.
38. van Breemen, R.B., and Li, Y. (2005). Caco-2 cell permeability assays to measure drug absorption. *Expert Opin. Drug Metab. Toxicol.* *1*, 175–185.
39. Qu, F., Ai, Z., Liu, S., Zhang, H., Chen, Y., Wang, Y., and Ni, D. (2021). Study on mechanism of low bioavailability of black tea theaflavins by using Caco-2 cell monolayer. *Drug Deliv.* *28*, 1737–1747.
40. Ahmed, I., Leach, D.N., Wohlmuth, H., De Voss, J.J., and Blanchfield, J.T. (2020). Caco-2 Cell Permeability of Flavonoids and Saponins from *Gynostemma pentaphyllum*: the Immortal Herb. *ACS Omega* *5*, 21561–21569.
41. Degim, Z., Unal, N., Essiz, D., and Abbasoglu, U. (2005). Caco-2 cell culture as a model for famotidine absorption. *Drug Deliv.* *12*, 27–33.
42. Juliano, R.L., Ming, X., and Nakagawa, O. (2012). Cellular uptake and intracellular trafficking of antisense and siRNA oligonucleotides. *Bioconjug. Chem.* *23*, 147–157.
43. Juliano, R.L., Ming, X., Carver, K., and Laing, B. (2014). Cellular uptake and intracellular trafficking of oligonucleotides: implications for oligonucleotide pharmacology. *Nucleic Acid Ther.* *24*, 101–113.
44. Wang, Z., Feng, Y., Song, T., Su, J., Fu, M., and Lei, H. (2021). Study on the interaction of *Zea mays* L. centrin and melittin. *RSC Adv.* *11*, 36098–36104.
45. Crooke, S.T., Baker, B.F., Crooke, R.M., and Liang, X.H. (2021). Antisense technology: an overview and prospectus. *Nat. Rev. Drug Discov.* *20*, 427–453.
46. Kierzek, E., and Kierzek, R. (2003). The thermodynamic stability of RNA duplexes and hairpins containing N6-alkyladenosines and 2-methylthio-N6-alkyladenosines. *Nucleic Acids Res.* *31*, 4472–4480.
47. Roost, C., Lynch, S.R., Batista, P.J., Qu, K., Chang, H.Y., and Kool, E.T. (2015). Structure and thermodynamics of N6-methyladenosine in RNA: a spring-loaded base modification. *J. Am. Chem. Soc.* *137*, 2107–2115.
48. Chen, X., Li, A., Sun, B.-F., Yang, Y., Han, Y.-N., Yuan, X., Chen, R.-X., Wei, W.-S., Liu, Y., Gao, C.-C., et al. (2019). 5-methylcytosine promotes pathogenesis of bladder cancer through stabilizing mRNAs. *Nat. Cell Biol.* *21*, 978–990.
49. Chen, Y., Zuo, X., Wei, Q., Xu, J., Liu, X., Liu, S., Wang, H., Luo, Q., Wang, Y., Yang, Y., et al. (2023). Upregulation of LRRC8A by m(5)C modification-mediated mRNA stability suppresses apoptosis and facilitates tumorigenesis in cervical cancer. *Int. J. Biol. Sci.* *19*, 691–704.
50. Yang, M., Wei, R., Zhang, S., Hu, S., Liang, X., Yang, Z., Zhang, C., Zhang, Y., Cai, L., and Xie, Y. (2023). NSUN2 promotes osteosarcoma progression by enhancing the stability of FABP5 mRNA via m(5)C methylation. *Cell Death Dis.* *14*, 125.
51. Zheng, L., Yang, T., Guo, H., Qi, C., Lu, Y., Xiao, H., Gao, Y., Liu, Y., Yang, Y., Zhou, M., et al. (2024). Cryo-EM structures of human SID-1 transmembrane family proteins and implications for their low-pH-dependent RNA transport activity. *Cell Res.* *34*, 80–83.
52. Lubini, P., Zürcher, W., and Egli, M. (1994). Stabilizing effects of the RNA 2'-substituent: crystal structure of an oligodeoxynucleotide duplex containing 2'-O-methylated adenosines. *Chem. Biol.* *1*, 39–45.
53. Parhiz, H., Atochina-Vasserman, E.N., and Weissman, D. (2024). mRNA-based therapeutics: looking beyond COVID-19 vaccines. *Lancet* *403*, 1192–1204.
54. Dhuri, K., Bechtold, C., Quijano, E., Pham, H., Gupta, A., Vikram, A., and Bahal, R. (2020). Antisense Oligonucleotides: An Emerging Area in Drug Discovery and Development. *J. Clin. Med.* *9*, 2004.
55. Hald Albertsen, C., Kulkarni, J.A., Witzigmann, D., Lind, M., Petersson, K., and Simonsen, J.B. (2022). The role of lipid components in lipid nanoparticles for vaccines and gene therapy. *Adv. Drug Deliv. Rev.* *188*, 114416.
56. O'Driscoll, C.M., Bernkop-Schnürch, A., Friedl, J.D., Prétat, V., and Jannin, V. (2019). Oral delivery of non-viral nucleic acid-based therapeutics - do we have the guts for this? *Eur. J. Pharm. Sci.* *133*, 190–204.